Eur. Phys. J. B **47**, 85–91 (2005)
DOI: 10.1140/epjb/e2005-00292-2

THE EUROPEAN PHYSICAL JOURNAL B

Damage growth in random fuse networks

F. Reurings and M.J. Alava[a]

Helsinki University of Technology, Laboratory of Physics, P.O. Box 1100, 02015 HUT, Finland

Received 28 January 2004 / Received in final form 6 May 2005
Published online 21 September 2005 –

Abstract. The correlations among elements that break in random fuse network fracture are studied, with disorder strong enough to allow for volume damage before final failure. The growth of microfractures is found to be uncorrelated above a lengthscale, that increases as the final breakdown approaches. Since the fuse network strength decreases with sample size, asymptotically the process resembles more and more mean-field-like ("democratic fiber bundle") fracture. This is found from the microscopic dynamics of avalanches or microfractures, from a study of damage localization via entropy, and from the final damage profile. In particular, the last one is statistically constant, except exactly at the final crack zone, in spite of the fact that the fracture surfaces are self-affine. This also implies that the correlations in damage are not extensive.

PACS. 62.20.Mk Fatigue, brittleness, fracture, and cracks – 62.20.Fe Deformation and plasticity (including yield, ductility, and superplasticity) – 05.40.-a Fluctuation phenomena, random processes, noise, and Brownian motion – 81.40.Np Fatigue, corrosion fatigue, embrittlement, cracking, fracture and failure

1 Introduction

The scaling properties of fracture processes continue to attract interest from the statistical mechanics community. Key quantities are the geometric properties of fracture surfaces and statistics of acoustic emission, or, in analogy to other systems, "crackling noise". The point is that in failure of brittle materials the elastic energy of a sample is released in bursts. These "avalanches" often turn out to have scale-invariant statistics with respect to e.g. the probability distribution of the released energy [1–5]. Likewise, crack surfaces are often self-affine (with an empirical roughness exponent ζ) [6–8]. The understanding of the origins of such critical-like statistics would perhaps be of interest to engineers ("how to make tougher materials") but would also mean the solution of a very complicated many-particle system.

In this respect, among the simplest models that are available are mean-field like fiber bundle models (FBM) [9,10] and random fuse networks (RFN's) [11,12]. The former describe democratic or global load sharing, and thus do not have anything close to the stress enhancements of real cracks (though one can introduce local load sharing to fiber bundles, and interpolate between these two limits as well). Such stress effects are to be found in a natural way in fuse networks that simplify real elasticity by considering the electrostatic analogy. RFN's have two fundamental limits: weak disorder, when cracks are nucleated quickly and brittle failure takes place without much precursor activity, and strong disorder (without infinitely strong elements), where *damage* develops before macroscopic failure [11,13].

The above mentioned two signatures are found in the latter, RFN, case, that also characterize experimental systems: rough, self-affine cracks and microcracking that corresponds to the acoustic emission. The roughness exponent is in the proximity of $\zeta_{RFN} \sim 0.7 \ldots 0.75$, in 2d, tantalizingly close to the minimum energy surface exponent, exactly 2/3. This result holds also for e.g. 'weak' disorder [14–16] and is close to what is seen in experiments [17–20]. The damage develops in avalanches [10,5,21,22], in analogy to democratic FBM's [23], or what we in the following call the "mean-field limit" (MF-). In the FBM case one would have for the probability distribution of the number of fuses (Δ) blown in one 'event', for current-control,

$$P(\Delta) \sim \Delta^{-5/2}. \quad (1)$$

The corresponding AE energy exponent seems to be about $\beta = 1.7$ [5,24,22], as would be expected based on the exponent relation $\beta = (5/2+1)/2$ [24]. Note however that the RFN exponent is not exactly 5/2 but slightly higher and thus the theoretical situation remains partly open [22]. However, even for strong disorder finally stress enhancements come into play, and the sample fails catastrophically, with the elastic modulus (conductivity, in the RFN case) having a first-order drop.

[a] e-mail: mja@fyslab.hut.fi

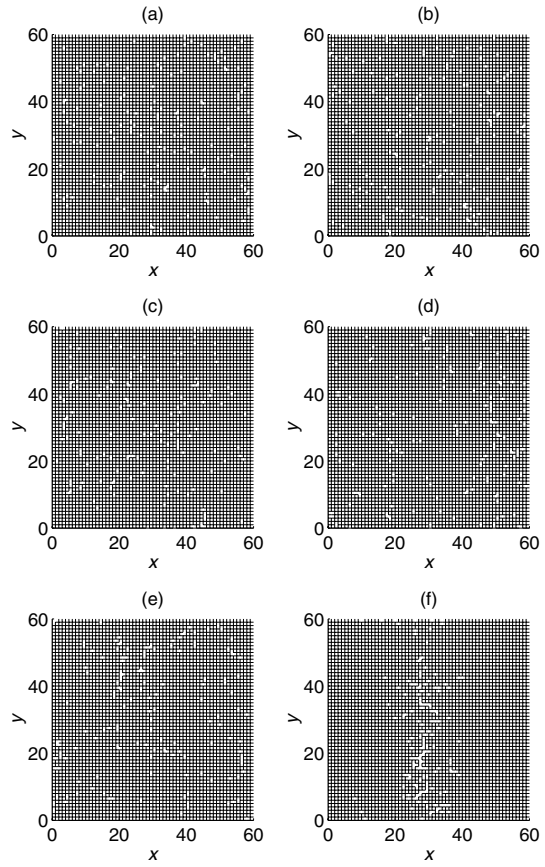

Fig. 1. Snapshots of subsequent damage patters in a failure of a RFN (each sub-plot having the same number of failed fuses, separately). $R = 1$, "strong disorder", $L = 60$.

The purpose of this article is to investigate the development of the damage, between the MF-limit valid at the very initial stages of fracture and the final critical crack growth. Figure 1 shows an example of the transition. We use for the failure thresholds of the fuses, i_c, a flat distribution $P(i_c) = [1-R, 1+R]$, with the disorder parameter R chosen as unity. The subplots depict the individual fuses that fail in subsequent parts of a stress-strain- (or current-voltage) history. Clearly, initially the damage is random (unless proven differently by more sophisticated analysis), and in the last panel it concentrates on the vicinity and at the final crack.

In this respect, it is an important question how the pre-critical damage reflects the self-affine properties of the final fracture surface. Recently, Hansen and co-workers have attempted to relate its formation to a self-consistently developed damage profile that extends over all the sample [25,26]. The scaling of the profile with the system size would then explain the roughness and its exponent. Clearly, this should also be visible in the dynamics of failure also prior to the end of the process. Another analogy is given by dynamics in dipolar random field magnets, which can account for the symmetry breaking (as signaled by the formation of the final crack) due to shielding in the direction of the external voltage and for stress enhancements that drive cracks mostly perpendicular to it [27].

We study these aspects by concentrating on two kinds of quantities: those that characterize the spatial distribution of damage in samples, and those that analyze the temporal correlations between subsequent, individual failure events (as e.g. during an avalanche, or series of fuse failures due to the increase of a control parameter). Section 2 considers the former, and uses entropy as the main tool. This compares the damage integrated over windows of time and/or space to that in, spatially, completely random damage formation. We also study the damage profiles of completely failed samples. From both kinds of analysis emerges a picture of crack development, which is mean-field -like beyond a finite interaction range (i.e. the failures are randomly distributed). This is true until the final breakdown is induced, related to as usual to rare event statistics [12]. This in particular includes the fact that except in the "fracture process zone", i.e. in the vicinity of the final crack, the damage is statistically homogeneous. Thus in this particular case of RFN's the theory proposed by Hansen et al. seems unlikely to be the explanation for the self-affine geometry of cracks.

In Section 3, the internal dynamics of avalanches is considered. We look at the probability distributions and average values of "jumps" (relative changes in the position of subsequent failures). It transpires that there is a smooth development, in which the these quantities exhibit a cross-over from the FBM/MF-like lack of spatial inhomogeneity towards localized crack growth within a scale ξ. This resembles some observations by Curtin about critical damage clusters in a more elaborate fiber bundle-type model: the scaling of strength is based on democratic load sharing in spite of the presence of stress enhancements [28]. It also pertains to the question of the existence of "representative volume elements" [29] or coarse-graining in fuse networks [30], related to the general question of how to account for microscopic dynamics and phenomena with coarse-grained variables and equations. Beyond any such correlation length ξ as may be defined within avalanches the network looks homogeneous, and this is in particular true if in addition the damage density is statistically homogeneous. Finally, we finish the paper in Section 4 with a summary and some open prospects.

2 Distribution of damage

The RFN's, as electrical analogues of (quasi-)brittle media consist of fuses with a linear voltage-current relationship until a breakdown current i_b. A stress-strain test can be done by using adiabatic fracture iterations: the current balance is solved, and at each round the most strained fuse is chosen according to $\max(i_j/j_{c,j})$, where i_j is the local current and $j_{c,j}$ the local threshold). Currents and voltages are solved by the conjugate-gradient method. The simulations are done in 2d, in the (10) square lattice orientation, with periodic boundary conditions in the transverse direction (y) and the current flow in the other. Square systems upto 100^2 have been studied; notice that the damage is in practice volume-like, and thus thousands of iterations are needed per a single system for $L \sim 100$.

We create series of subsequent fuse failures for each system, and extract from these the current- or voltage-driven cases according to the case at hand (note that this choice only affects the distribution to avalanches, and the VI-curve).

Studies of the break-down current I_b as a function affirm the expected outcome of a logarithmic scaling [12,16] as a function of L, resulting from extremal statistics ($I_b \sim L/\ln L$). This implies in the mean-field limit that $n_b \sim \frac{L^2}{\log L}$, where n_b is the average number of broken fuses in a system.

To analyze the spatial of distribution of damage it is useful first to take note of the fact that in the latter stages the system behaves anisotropically: just before the formation of a critical crack the spatial density of the broken fuses should be a stochastic variable, with a constant mean in the transverse direction to the external voltage. However, along the voltage direction differences may ensue. To study such trends in the damage mechanics and the localization we consider the entropy of the damage averaged over y in each sample (this is in analogy to the procedure used with AE experiments, of Guarino et al. [3]). The network is divided along the current flow direction into sections, and the entropy S defined as

$$S = -\sum_i q_i \ln q_i, \tag{2}$$

where q_i is the fraction of burned fuses in section i. S is normalized by S_e, the entropy of a random, on the average homogeneous distribution of failures (of equal total damage). Thus the extreme limits are zero and unity, corresponding to completely localized damage and complete random one, respectively. The final crack extends between $y = 0$ and $y = L$, and a sensible choice is to use for the section width δx a value larger than the typical interface width w,

$$w = \langle (h_y - \bar{h})^2 \rangle^{1/2}, \tag{3}$$

where h_y denotes the crack location and $\bar{h}$ its mean position in the x-direction. Since $w \sim L^\zeta$, with $\zeta < 1$, it is clear that using a constant number of sections will with increasing L localize the fracture zone either entirely inside one, or between two neighboring ones. For better statistics it is preferable to have $\delta x \gg 1$, though the interpretation is perhaps more difficult than for the extreme value $\delta x = 1$, say. The width of the sections used in computing the entropies was chosen to be $\delta x = L/10$.

In this discrete form, the entropy reads

$$S = -\sum_{i=1}^{k} \frac{n_i}{N} \ln \frac{n_i}{N}, \tag{4}$$

where $k = L/\delta x$ is the number of sections, n_i the number of burnt fuses in the i'th section, and $N = \sum_{i=1}^{k} n_i$ is again the total number of fuses. Note that the absolute value of S is dependent on the choice for δx. S can now be used to consider different parts of the stress-strain curve, separately, or the final damage pattern.

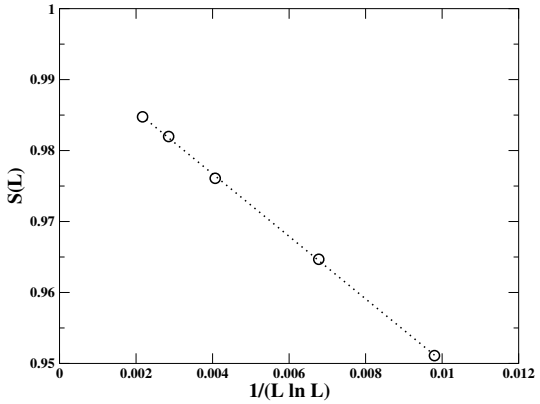

Fig. 2. S vs. $1/(L \log L)$ in networks with strong disorder ($R = 1$). The straight line is a linear least squares fit that intersects the S-axis at $S = 0.9943$.

Figure 2 shows the total entropy versus system size. The best kind of linearity with respect to the data is obtained with a scaling variable $1/(L \log L)$. This can be considered with the following Ansatz. Assume that the fractures are distributed otherwise randomly ($n_{b,i}$), except the one containing the final crack, which has $n_{b,k} + \Delta n_{b,k}$ where k is its section. Take $\Delta n_b \ll \langle n_b \rangle$, which implies approximately $S \approx 1 - \ln k(\Delta n_{b,k}/n_b)$. Noticing the logarithmic scaling of damage, it follows that $S \sim -1/(L \log L)$, if and only if $\Delta n_{b,k}$ scales as $\Delta n_{b,k} \sim L/(\log L)^2$. We have not checked explicitly that this holds; note that the fracture surface, being self-affine, is thus supposed to contain L^a fuses, with $1 < a \ll 2$, but the fracture process zone contains other damage (broken fuses) contributing to Δn_b (see Fig. 1 again, and the last panel in particular). In any case, it is obvious that the entropy *increases* with system size, indicating more and more completely random damage. The limiting value of S is slightly below unity; here it is hard to say whether this difference is due to the choice used for computing S or a real one [31].

In Figure 3 an example is shown of how the damage actually localizes when the fracture process is divided into sequential slices, i.e. by taking a fixed number of consecutive fuse failures for each. It is clear that initially most of the fuses break randomly, and only in the last one strong localization takes place. Similar sampling can also be done with the external voltage or current as control parameters, the difference between these two being that the final avalanches are different (the fracture is more abrupt in the current-driven case and thus the final avalanche is larger).

This lack of the localization of damage is reflected in Figures 4 and 5. The first one shows three examples of the damage profiles $\rho(x)$ where the average is simply performed over the perpendicular direction for each separately. In Figure 5, the damage density $\langle \rho \rangle(\chi)$ is averaged in the y-direction over the number of fuses that fail at fixed position, as a function of the normalized coordinate transform $\chi = (x - x_c + L)/2L$. Here the point x_c is chosen as the one with the maximum damage, and is located in practice at the final fracture line, $x_c \simeq \bar{h}$. Notice that it is imperative that x_c is chosen to be inside the

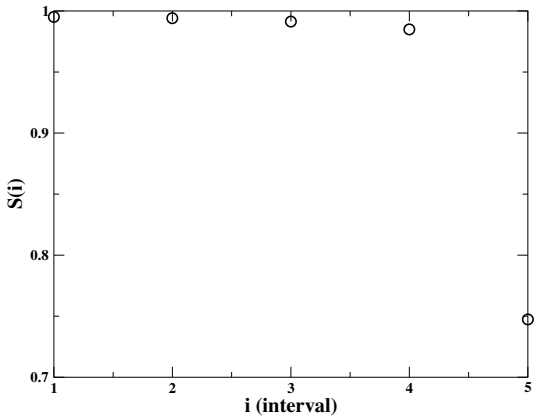

Fig. 3. Entropy S versus time interval Δn_i. $L = 100$, $R = 1$. Average over 20 realizations.

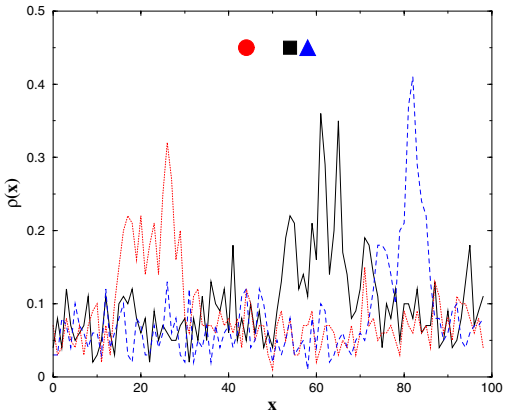

Fig. 4. The damage density $\langle\rho\rangle(x)$ along the current direction (averaged over the perpendicular direction) for three random samples. One can see the rough locations of the final cracks. Moreover, the plot also demonstrates the locations of the center-of-masses of the three samples (circle: dotted case; square: solid case; triangle: dashed one) Here $L = 100$, $R = 1$.

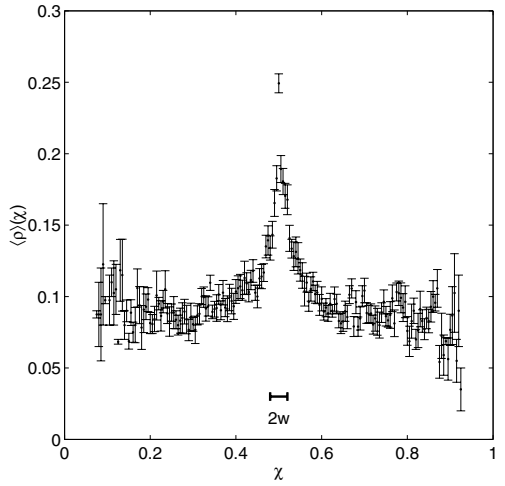

Fig. 5. Averaged damage density $\langle\rho\rangle(\chi)$. $L = 100$, $R = 1$.

sample-dependent crack zone. Using for instance a damage center-of-mass for it would confuse the issue, since for e.g. $L = 100$ most of the damage is located outside of this zone, and the truly localized part of the density of broken fuses is not detected properly, using such a definition (consider again Fig. 1.). This can be seen in Figure 4: the background (of damage which fluctuates and is uncorrelated on the scale of the system, L) obscures the location of the crack. Due to the diffuse nature of the crack and the fact that $\zeta < 1$ this becomes only worse with increasing L.

After this shift, the average density is computed taking care that it is normalized correctly since the number of samples contributing for each χ varies with the final crack location – x_c is a random variable. We also have added the average fracture line width $w(L = 100)$ as a comparison (from Ref. [16]). It can be seen that outside of the immediate vicinity of the fracture process zone the damage is constant. Notice the error bars of the data points, and that the data points located far away from the crack line suffer from the presence of less data points as seen from the error bars. It would be interesting to analyze in detail the functional shape of $\langle\rho\rangle(\chi)$ in the proximity of the crackline, $\chi = 0.5$. The implication of the results is that the density can be written as a sum of a constant (L-dependent) background, and a term that has to decay (perhaps exponentially) within a finite lengthscale from the crack. This decay length in turn may depend on L. In reference [32] it has been pointed out that the best way to address the averaging this to subtract first the data *before the peak stress* and look thus only at the damage in the post-maximum phase. Then, one can use the center-of-mass -shift to superimpose the damage profiles. However, the same authors also emphasized the absence of a correlated damage profile both before the current maximum, and in the post-maximum case outside of the crack zone itself. This agrees with the impression Figure 5 gives.

Such an observation is in contradiction to the proposed "self-consistent" quadratic functional form, by Hansen et al. [14]. This would imply $\langle\rho\rangle(\chi) = p_f - A\left(\frac{L(2\chi-1)}{l_x}\right)^2$, where p_f is the maximum density; this is clearly not the case. In the light of the picture discussed below about the internal dynamics of microcracks or avalanches, the interpretation is that the final crack is formed here similarly to weak disorder in a "critical" manner. That is, once a damage density sufficient for "nucleation" is established the largest crack becomes unstable. Prior to that the correlations in the damage accumulated can for all purposes be neglected. This would in turn to imply that the origin of the self-affine crack roughness in fuse networks is *not dependent* on whether there is "strong" or "weak" disorder, as long as there are no infinitely strong fuses, or as long as the process does not resemble e.g. percolation due to the complete domination of zero-strength fuses.

3 Avalanches

Next we consider the correlations in the dynamics of individual fuse failures. Recall that the MF-limit states that consecutive ones should not be spatially correlated in any

fashion; the opposite limit is given by the growth of a linear crack in which it is always the one adjacent to the crack tip to fail next. In the case that the growing crack is "rough" one expects that the subsequent failure takes place inside a fracture process zone, analogously to normal fracture mechanics, one of the follow-up questions being how the size and the shape of this zone vary with system size and as the crack grows [15]. The simplest quantities to compute, to examine localization and spatial correlations between fractures, are the 1d distances between consecutive fractures,

$$\Delta x = |x_{i+1} - x_i| \tag{5}$$

$$\Delta y = |y_{i+1} - y_i|, \tag{6}$$

where x_i and y_i are the x- and y-coordinates of the ith fracture. Another one choice is given by the average distances between consecutive fractures belonging to the same avalanche (i.e. induced by a single increment of the control parameter)

$$\Delta x_{avalanche} = \frac{1}{\Delta - 1} \sum_{i=1}^{\Delta-1} |x_{i+1} - x_i| \tag{7}$$

$$\Delta y_{avalanche} = \frac{1}{\Delta - 1} \sum_{i=1}^{\Delta-1} |y_{i+1} - y_i|. \tag{8}$$

Here Δ is the avalanche size, in fuses failed. The MF (FBM or random -like damage) theory predicts $P(\Delta x = k) = 2(L-k)/L^2$ and $P(\Delta y = k) = 2/L$, if the boundary conditions used here are taken into account, and Δ is again the avalanche size measured in the number of fuses broken during it. For clarity note that we are here assuming "democratic load sharing": the positions would be located randomly.

Figure 6 depicts, as a comparison for the mean-field results, the average distances in the x- and y-dimensions between consecutive broken fuses belonging to the same avalanche. $\langle \Delta x_{avalanche} \rangle$ and $\langle \Delta y_{avalanche} \rangle$, are shown, respectively, as a function of the system size. Both are linear like in the MF theory, but with a smaller slope with L. This means, that the damage created by a typical avalanche (microcrack creation, crack advance etc.) *is localized* compared to the MF-prediction, but nevertheless the localization does not get stronger with L. One should note that the damage as such is almost volume-like. The result is thus not surprising in the sense that a reduction of the slope (sublinear behavior, say, $\langle \Delta x_{avalanche} \rangle \sim L^{\alpha}$, with $\alpha < 1$) would imply concomitant faster average crack growth, which would be in contradiction with the damage scaling.

To understand the dynamics of microcracks in detail is a difficult task. This is since the growth dynamics is not local: the burned fuses do *not* have to form connected clusters by any remotely easy criterion. It is easy to comprehend that the driving force for the localization is standard stress-enhancement, but as is true for RFN's crack shielding and arrest (due to strong fuses, in the early stages of fracture) play a role. One may set aside for the sake of discussion the separation of the events into avalanches, and just consider the distances between consecutive burned fuses. Figure 7 demonstrates the difference between two probability distributions $P(\Delta x)$, averaged over the first 1/8 of the typical failure process and the last, respectively, for a fixed L. As one could expect, there is a peak in the distribution (this holds for both x- and y-directions separately), which is greatly suppressed in the first part closest to the MF-limit.

Thus one may conclude that there is a continuous cross-over from purely MF-like behavior to a complicated non-local growth dynamics. This is also exhibited by such distributions $P(\Delta x)$, $P(\Delta y)$. The analysis of the detailed shape of the small-argument part of the probability distributions would be an interesting challenge. To first order, the result is a convolution of a microcrack size distribution

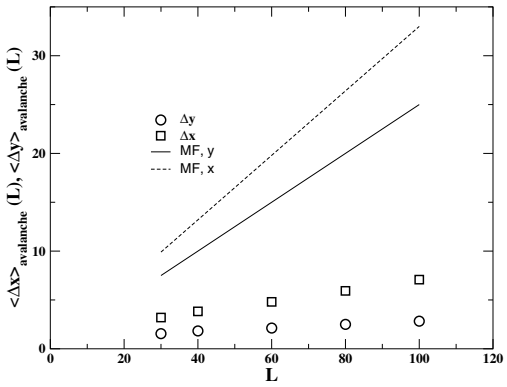

Fig. 6. Average one-dimensional distances $\langle \Delta x_{avalanche} \rangle$ and $\langle \Delta y_{avalanche} \rangle$ between consecutive broken fuses belonging to the same avalanche vs. linear dimension of system L. $R = 1$. The solid lines are linear least squares fits with slopes 0.018 for $\langle \Delta x_{avalanche} \rangle$ and 0.055 for $\langle \Delta y_{avalanche} \rangle$. The dashed lines, linear with slopes 0.33 for $\langle \Delta x_{avalanche} \rangle$ and 0.25 for $\langle \Delta y_{avalanche} \rangle$, correspond to the distances predicted by mean-field theory. Statistical errors are smaller than or equal to the size of the data points.

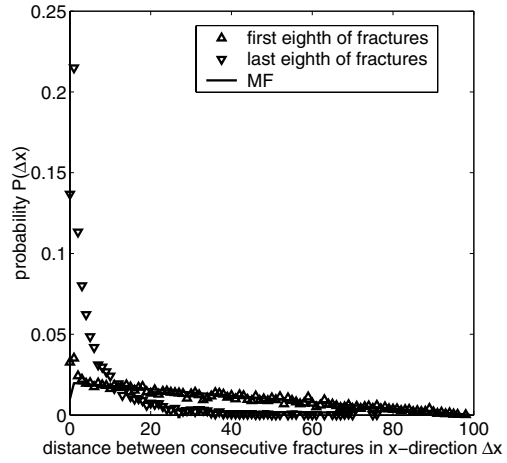

Fig. 7. Distribution of average distances in the x-dimension between consecutive broken fuses computed over the 1st and 8th 8th of the fractures of 20 realizations. $L = 100$, $R = 1$. The solid lines correspond to mean-field predictions.

and the corresponding stress enhancement factor, such that the distribution P evolves or grows according to the underlying probability distribution of crack sizes and locations. Given the simple forms of say $P(\Delta x)$ for small arguments there might be some hope for developing analytical arguments.

When considered as a function of L it becomes immediately apparent why the avalanche statistics resembles the MF-case so much. This is due to two separate factors: first, the growth is clearly in the sample case of Figure 7 (or Fig. 1 again) local over a certain lengthscale (damage correlation length), ξ_x or ξ_y. Second, one should recall the scaling of the strength with L: catastrophic crack growth takes place earlier and earlier with respect to the intensive variable, current. This means that the RFN's resemble, in the thermodynamic limit, more and more the mean-field-case in their fracture properties in spite of the stress- (or more exactly current-) enhancements that the model contains.

Again, our data does not allow us to conclude firmly how such correlation lengths behave for small Δx or Δy - how the associated distributions P would scale for small arguments that is. This is due to the limited scaling range of P (at least for the given disorder, but of course $\xi_y \ll L$ as well). One may however simply use an Ansatz that $P \sim \Delta y^{-\tau}$ upto ξ_y, say and MF-like for larger Δy [30]. This defines the correlation length ξ_y for a given damage density ρ. Using now such a distribution P allows to compute $\langle \Delta y \rangle$ and relate it to ξ_y. This approach is valid for fracture processes that deviate from uncorrelated ones for scales such that $\xi_y \ll \langle L/4 \rangle$. The result is in analogy to Delaplace et al. [30] that for a given damage level,

$$\langle \Delta y \rangle = \frac{1-\tau}{4(2-\tau)} \frac{(2-\tau)L^2 + 8\tau\xi_y^2}{(1-\tau)L + 2\tau\xi_y}. \qquad (9)$$

This defines implicitely ξ_y, with the aid of $\langle \Delta y \rangle$. In the opposite limit, $\xi_y \sim 1$ the correlations are badly defined since the model discretization comes into play. Figure 8 shows an example of the ensuing scaling with different guesses for τ, for $L = 100$. The main observation is an exponential (perhaps) increase of ξ_y with damage. Again, note that with still larger system sizes the total damage is diminished, which in turn implies that the maximal correlations in the damage accumulation become weaker. Please observe that we have not studied in detail the other possibility, ξ_x since the main interest lies with the correlations in the crack-growth direction.

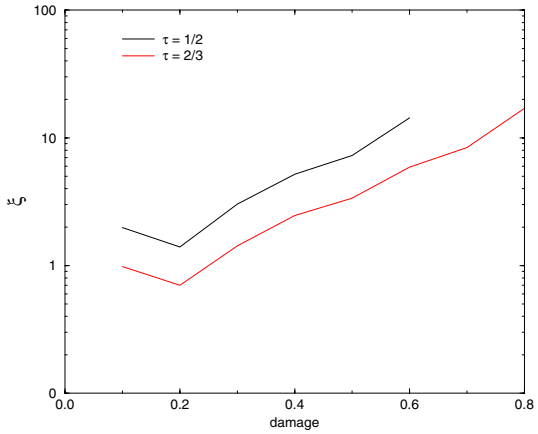

Fig. 8. The scaling of ξ_y (see Eq. (9)) with increasing damage for $L = 100$. The total number of broken bonds has been divided into ten consecutive windows, and in each of these $\langle \Delta y \rangle$ has been computed, and ξ_y using equation (9). For τ two guesses (1/2, 2/3) are used, note that $0 < \tau < 1$.

4 Summary

In this article we have studied the distributions and development of damage in random fuse networks, with "strong" disorder. Our aim has been to understand possible deviations from mean-field theory, and the associated correlations. This is of relevance both as regards the statistical mechanics of fracture in general, and in particular also the growth and formation of self-affine cracks. In other words, we have concentrated on the "approach to the critical point" if the failure transition is considered as an analogue of ordinary phase transitions.

An analysis of the localization of damage both during the fracture process and a posteriori reveals that in the case studied the correlations are very weak, are formed mostly in the last catastrophic phase of network failure, after the maximum current I_{max}, and do not have any global correlations. The localization is centered in and around the final crack surface, or what may be called as the total volume encompassed by a "fracture process zone". We would like to note that this is in contrast to the recent theory of self-organized damage percolation, of Hansen et al. ([25]) devised to explain the formation of self-affine cracks in fuse networks, and in related experiments. In particular it should be stressed that there is no evidence of a global, non-trivial damage profile as implied by that proposition – the only localization can be found in the immediate vicinity of the crack. Recent numerical results of Nukala et al. [32] with much better statistics than what is the case here or with the works of other, earlier authors, also imply the same.

Since also in this particular case much of the damage incorporated in the final crack is due to the "last" avalanche it seems then logical that the fracture surface geometry is formed similarly to RFN's *with weak disorder*, for which there is no quasi-volume like damage, and one often has just the propagation, and formation of the final crack. In spite of this difference in the amount of damage, the measured roughness exponents from such simulations are close; this seems to imply that it is the correlated growth in the final, unstable crack formation that gives rise to the self-affine properties.

The internal correlations of the avalanches become more and more important as damage grows, but in line with the fact that the statistics is close to the mean-field case the growth is never very far from the MF-case: for all phases studied there are subsequent remote broken fuses,

so that there is no complete localization, even very close to the last growth event. There is an associated localization engthscale that can be roughly defined based on the x- and y-dependent results, but of course one could go further and look at the radial probability distribution $P(\vec{r})$, with $\vec{r} = (x_{i+1}, y_{i+1}) - (x_i, y_i)$ (for which one would presumably need still much larger systems to get decent averaging). One central lesson is that localization will diminish with system size due to the normal volume effect of strength, decreasing with L. In this respect, fuse networks are not unique, and other simulation models of brittle fracture should exhibit the same behavior. To conclude, even in our case with quite strong disorder the failure process consists of weakly correlated damage growth and a final catastrophic crack propagation phase, that induces a first-order drop in the elastic modulus.

We are grateful to the Center of Excellence program of the Academy of Finland for support.

References

1. D.A. Lockner et al., Nature **350**, 39 (1991)
2. A. Petri, G. Paparo, A. Vespignani, A. Alippi, M. Costantini, Phys. Rev. Lett. **73**, 3423 (1994)
3. A. Guarino, A. Garcimartin, S. Ciliberto, Eur. Phys. J. B **6**, 13 (1998); A. Garcimartin et al., Phys. Rev. Lett **79**, 3202 (1997)
4. L.C. Krysac, J.D. Maynard, Phys. Rev. Lett. **81**, 4428 (1998)
5. L.I. Salminen, A.I. Tolvanen, M.J. Alava, Phys. Rev. Lett. **89**, 185503 (2002)
6. B.B. Mandelbrot, D.E. Passoja, A.J. Paullay, Nature (London) **308**, 721 (1984)
7. E. Bouchaud, J. Phys.: Condens. Matter **9**, 4319 (1997)
8. P. Daguier, B. Nghiem, E. Bouchaud, F. Creuzet, Phys. Rev. Lett. **78**, 1062 (1997)
9. M. Kloster, A. Hansen, P.C. Hemmer, Phys. Rev. E **56**, 2615 (1997)
10. S. Zapperi et al., Phys. Rev. Lett. **78**, 1408 (1997)
11. Chapters 4–7 in *Statistical models for the fracture of disordered media*, edited by H.J. Herrmann, S. Roux (North-Holland, Amsterdam, 1990)
12. P.M. Duxbury, P.L. Leath, P.D. Beale, Phys. Rev. B **36**, 367 (1987); P.M. Duxbury, P.L. Leath, P.D. Beale, Phys. Rev. Lett. **57**, 1052 (1986)
13. B. Kahng, G.G. Batrouni, S. Redner, L. de Arcangelis, H.J. Herrmann, Phys. Rev. B **37**, 7625 (1988)
14. A. Hansen, E.L. Hinrichsen, S. Roux, Phys. Rev. Lett. **66**, 2476 (1991)
15. V. Räisänen, M. Alava, E. Seppälä, P.M. Duxbury, Phys. Rev. Lett. **80**, 329 (1998)
16. E.T. Seppälä, V.I. Räisänen, M.J. Alava, Phys. Rev. E **61**, 6312 (2000)
17. J. Kertész, V.K. Horvath, F. Weber, Fractals **1**, 67 (1993)
18. T. Engoy, K.J. Maloy, A. Hansen, Phys. Rev. Lett. **73**, 834 (1994)
19. J. Rosti et al., Eur. Phys. J. B **19**, 259 (2001)
20. L.I. Salminen, M.J. Alava, K.J. Niskanen, Eur. Phys. J. B **32**, 369 (2003)
21. S. Zapperi, P. Ray, H.E. Stanley, A. Vespignani, Phys. Rev. E **59**, 5049 (1999)
22. S. Zapperi, P.K.V.V. Nukala, S. Simunovic, Phys. Rev. E **71**, 026106 (2005)
23. For 3d RFN's the situation is not so clear-cut: V.I. Räisänen, M.J. Alava, R.M. Nieminen, Phys. Rev. B **58**, 14288 (1998)
24. M. Minozzi, G. Caldarelli, L. Pietronero, S. Zapperi, Eur. Phys. J. B **36**, 203 (2003)
25. A. Hansen, J. Schmittbuhl, Phys. Rev. Lett. **90**, 045504 (2003)
26. T. Ramstad, J.O.H. Bakke, J. Bjelland, T. Stranden, A. Hansen, e-print `cond-mat/0311606`
27. M. Barthelemy, R. da Silveira, H. Orland, Europhys. Lett. **57**, 831 (2002)
28. W.A. Curtin, Phys. Rev. Lett. **80**, 1445 (1998)
29. P. Van, C. Papenfuss, W. Muschik, Phys. Rev. E **62**, 6206 (2000)
30. A. Delaplace, G. Pijaudier-Cabout, S. Roux, J. Mech. Phys. Solids **44**, 99 (1996)
31. Since the original version of the manuscript was submitted to the cond-mat preprint archive, the entropy analysis has also been used for much larger ensembles of RFN data; the results support the picture of uncorrelated damage (P.K.V.V. Nukala, personal communication)
32. P.K.V.V. Nukala, S. Simunovic, S. Zapperi, J. Stat. Mech. Theo. Expt., P08001 (2004)